JOURNAL OF THERMOPHYSICS AND HEAT TRANSFER
Vol. 14, No. 2, April–June 2000

Determination of Spectral Radiative Properties of Open Cell Foam: Model Validation

D. Baillis,* M. Raynaud,† and J. F. Sacadura‡
Centre National de la Recherche Scientifique, 69621 Villeurbanne Cedex, France

Spectral radiative properties (absorption coefficient, scattering coefficient, and phase function) of open cell carbon foam are determined experimentally. The identification method uses spectral transmittance and reflectance measurements and a prediction model based on a combination of geometric optics laws and of diffraction theory. In the wavelength region of 0.1–2.1 μm, directional–hemispherical transmittance and reflectance measurements are used, whereas directional–directional transmittance and reflectance measurements are used in the wavelength region of 2–15 μm. Thus, radiative properties are determined in the wavelength region from visible to infrared. The two approaches corresponding to the two different types of measurement (directional–directional and directional–hemispherical) are compared for the determination of radiative properties. Moreover, experiments performed on a guarded hot-plate-type device are used to confirm that the proposed model is appropriate to predict the radiative heat transfer in such media.

Nomenclature

b = minimum thickness of strut (Fig. 1)
$b_{\max}$ = maximum thickness of strut (Fig. 1)
fs = fraction defined by the following relation: strut cross-sectional area/area inscribed in a triangle defined by vertices of the strut
$\bar{G}_j$ = particle of type j ($j = 1, 2$) average geometrical cross section
ly = sample thickness
N_v = number of struts per unit volume
P_r = phase function due to reflection
α_λ = spectral volumetric absorption coefficient
β_R = Rosseland mean extinction coefficient
β_λ = spectral volumetric extinction coefficient
δ = porosity
θ = polar angle
ρ_λ = solid spectral hemispherical reflectivity
σ_λ = spectral volumetric scattering coefficient

I. Introduction

THERMAL radiation is the predominant mode of energy transfer in many engineering systems. A wide variety of these systems involve semitransparent media that are porous materials or media containing particulates that play a key role in the radiative transfer mechanisms. Some examples of these materials are soot, fibers, foams, reticulated ceramics, etc. An extensive review of radiative transfer in dispersed media was carried out by Viskanta and Mengüc[1] in 1989 and by Baillis and Sacadura[2] in 1997 with specific attention to advances that have been made since the beginning of the 1990s.

Open cell carbon foam can be used as efficient thermal insulation for high-temperature applications. Insulating foam consists of a highly porous solid material. Open cell foam insulations are semitransparent media (absorbing, emitting, and scattering radiation).

To model heat transfer in such media, it is necessary to determine radiative and conductive properties. In this work, a special emphasis is put on the determination of radiative properties of open cell carbon foam. The radiative properties of foam that are required for solving the radiative transfer equation are the spectral volumetric scattering and absorption coefficients and the spectral volumetric phase function. Recently, Baillis et al.[3] have adopted a new approach to determine such properties. Radiative properties were obtained from morphological data, such as porosity, particle sizes, and fs parameter, and from solid hemispherical reflectivity. Particle dimensions and porosity can be obtained from microscopic analysis, but solid hemispherical spectral reflectivities are very difficult to obtain directly. Baillis et al.[3] have determined solid hemispherical reflectivity and morphological parameter fs with an identification method. This method used spectral directional–directional experimental results of transmittance and reflectance obtained for several measurement directions and for several wavelengths in the range 2–15 μm. A good agreement was observed between experimental and theoretical results. These results are encouraging, but they do not permit validation of the model. Moreover, for high-temperature applications, it is necessary to determine radiative properties in the region of visible and near-infrared wavelengths. In this paper, a device with an integrating sphere is used to measure spectral directional–hemispherical transmittance and reflectance in the wavelength region of 0.2–2.1 μm.

The radiative properties predictive model and the identification method used to determine the unknown parameters are briefly described. Then application to a carbon foam sample of 98.75% porosity permits the study and validation of the model. This section represents the most innovative part of this work.

1) Sensitivity of different parameters (porosity, particle dimensions, etc.) on hemispherical reflectance and transmittance is studied.

2) Identification results obtained from the two approaches corresponding to two different types of measurements (hemispherical or directional) are compared to each other. The values of fs identified are also compared with the value of fs determined from a microscopic analysis.

3) Finally, experiments on a guarded hot-plate-type device allow comparison of the experimental and theoretical conductivities (accounting for radiative transfer, obtained from the radiative properties in the wavelength region of 0.2–15 μm). Results are also compared with simpler models that neglect scattering.

II. Predictive Model for Radiative Properties

Foam insulation such as reticulated porous ceramics are highly porous materials (porosity > 80%). Models and measurements for the radiative properties of such media have been presented by several

Received 29 July 1999; revision received 15 November 1999; accepted for publication 15 November 1999.

*Assistant Professor, Institut National des Sciences Appliquées de Lyon, Centre de Thermique de Lyon–UMR 5008; domino@cethil.insa-lyon.fr. Member AIAA.
†Professor, Institut National des Sciences Appliquées de Lyon, Centre de Thermique de Lyon–UMR 5008; raynaud@cethil.insa-lyon.fr.
‡Professor, Institut National des Sciences Appliquées de Lyon, Centre de Thermique de Lyon–UMR 5008; cethil@insa-lyon.fr.

different authors.[4–15] Inasmuch as Baillis and Sacadura[2] presented a review on the work devoted to the determination of radiative properties of such media, just a brief discussion is given here.

There are some works on the identification of radiative properties of such media from measurements. Extinction coefficient and scattering coefficient are identified by assuming a phase function of Henyey and Greenstein, or isotropic, or a combination of phase functions.[5,6,8,11,12] Very little work, however, has been done on the prediction of radiative properties from foam morphology and foam particles' dimensions. Foam radiative properties are difficult to quantify analytically because of their complex dodecahedral structure.

Glicksman et al.[13] considered the foam as a set of randomly oriented blackbody struts with constant thickness. They took an efficiency factor of one and neglected scattering phenomena.

Kuhn et al.[14] used infinitely long cylinders to model the struts. They converted the triangular cross sections into circular ones with the same area. Then they used Mie scattering calculations to predict the radiative properties.

The Doermann and Sacadura model[15] used in this work represents an improvement on previous ones. These authors consider particle modeling more representative of the actual geometry. It was obtained from the foam geometry description and from microscopic analysis of carbon open cell foams (Fig. 1). Struts with varying thickness and strut junctures were considered. The particles are assumed to have a random orientation and to be thick enough to be considered as opaque. Moreover, the scattering phenomena were accounted for by applying to these particles a combination of geometric optics and diffraction theory. Because of the extremely large values of the diffraction phase function in the forward direction ($\theta \approx 0$ deg), the diffraction contribution can be ignored; in the present study it is neglected. Application of geometric optics laws to the particles of the two types (particles of type 1 are struts, particles of type 2 are strut junctures) considered in this study leads to the following results:

$$\beta_\lambda = N_v(\bar{G}_1 + \bar{G}_2), \qquad \sigma_\lambda = \rho_\lambda N_v(\bar{G}_1 + \bar{G}_2)$$

$$\alpha_\lambda = (1 - \rho_\lambda)N_v(\bar{G}_1 + \bar{G}_2) \tag{1}$$

$$P_r(\theta) = (8/3\pi)(\sin\theta - \theta\cos\theta) \tag{2}$$

The phase function corresponding to reflection from a large opaque diffusely reflecting convex particle with random orientations is adopted by applying the following theorem[15,16]:

> The scattering pattern caused by a reflexion on a very large convex particle with random orientation is identical to the scattering pattern by reflexion on a very large sphere of the same material and surface condition.[16]

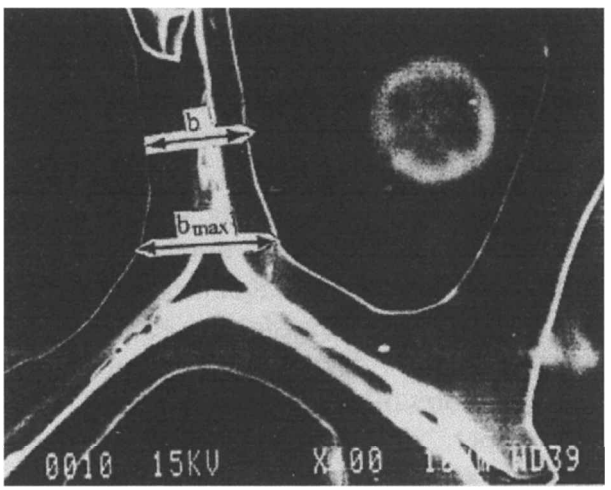

Fig. 1 Microscopical analysis obtained from carbon foam sample (magnification of 400); determination of dimensions b and b_{max} (Ref. 15).

Consequently, the radiative properties can be determined from the parameters ρ_λ, N_v, and $\bar{G}_j$, $j = 1, 2$. Doermann[17] has determined N_v and $\bar{G}_j$ as functions of the porosity δ, of the minimum and maximum thickness of the strut b and b_{max}, and of the parameter fs, defined as the fraction of the strut cross-sectional area to the area included in a triangle defined by the strut vertices.

The parameters b, b_{max}, and δ can be determined from microscopic analysis and photographs (Fig. 1). The main difficulty remains in the determination of ρ_λ. It cannot be obtained from direct measurement because the material needs to be compacted for this measurement. Moreover, it cannot be obtained reliably from the literature because of the great dispersion of the reported data. In previous work,[13] the fs value was taken as $\frac{2}{3}$. However, from microscopic analysis of different foam samples, it can be observed that fs seems to vary from one foam sample to another. Therefore Baillis et al.[3] have determined ρ_λ and fs by use of an identification method. The same approach is chosen in the current work.

III. Parameter Identification Method

This method uses experimental data of transmittances and reflectances T_{eij} obtained for several measurement directions i and for several measurement wavelengths j for a given set of samples and theoretical transmittances and reflectances T_{tij} calculated for the same directions and wavelengths as the experimental data and for the same sample thickness.

Baillis et al.[3] identified properties from directional–directional transmittance and reflectance by using a Fourier transform infrared spectrometer in the wavelength region of 2–15 μm.

In this study we use a Perkin Elmer Lambda 900 spectrometer with an integrating sphere attachment to acquire directional–hemispherical transmittance and reflectance measurements in the wavelength range of 0.2–2.1 μm. For the two cases, directional or hemispherical measurements, the technique is the same: The sample is submitted to a collimated near normal incidence beam. The spectral hemispherical reflectivity ρ_λ is discretized into nli points. A linear variation is assumed between two points. The goal is to determine the parameters fs and ρ_λ for nli wavelength, $\rho_{\lambda k}$, $k = 1$, nli, that minimize the quadratic differences F between the measured and calculated transmittances over the N measurement directions and NW measurement wavelengths:

$$F(\rho_{\lambda 1}, \ldots, \rho_{\lambda nli}, fs) = \sum_{j=1}^{NW}\sum_{i=1}^{N}[T_{tij}(\rho_{\lambda 1}, \ldots, \rho_{\lambda nli}, fs) - T_{eij}]^2 \tag{3}$$

The radiative transfer equation is solved using the discrete ordinates method with a quadrature over 24 directions. This quadrature allows a concentration of ordinates in the neighborhood of the incident direction. It has been adopted by Baillis et al.[3] and details are given therein. For the directional–directional measurements, the diffraction could not be neglected, especially for direction measurements near the normal. On the other hand, the diffraction can be ignored for the hemispherical measurements.

The number of parameters to identify is $n = nli + 1$. In the case of hemispherical measurements, the number of direction measurements is $N = 2$, one for transmittance and one for reflectance. For directional–directional measurements, $N = 7$ (two transmittances and five reflectances). For the two different types of measurements $NW = 230$. The method used in this work is the Gauss linearization method.[18] Because the reflectivity does not vary much, nli was chosen equal to 7. It represents a good compromise between speed and accuracy of the calculation. The ratio of the total number of measurements to the number of unknown parameters being large (for 230 wavelength measurements, this number is larger than 57) the identification method is appropriate. The seven wavelengths λi (μm) corresponding to the $\rho_{\lambda i}$ are given as follows: $\lambda 1 = 0.2$, $\lambda 2 = 0.25$, $\lambda 3 = 0.3$, $\lambda 4 = 0.4$, $\lambda 5 = 0.5$, $\lambda 6 = 0.7$, and $\lambda 7 = 2.1$.

IV. Application to a Carbon Foam Sample and Validation of the Model

A. Description of the Specimens

Foam porosity and particle dimensions obtained from a microscopical analysis are given as follows: $\delta \pm \Delta\delta = 98.75 \pm 0.78\%$, $b \pm \Delta b = 34 \pm 3\ \mu$m, and $b_{max} \pm \Delta b_{max} = 52 \pm 4\ \mu$m. To consider the medium as homogeneous, there must be sufficient pores in the thickness. Moreover, the thickness should not be too large otherwise there is no transmitted radiation. It seems to us that at least 10 pores is a reasonable compromise. The foam supplier indicated that the number of pores per inch was around 75 pores/in. ($\approx$3 pores/mm). Thus, four specimens of different thicknesses of the same foam are studied, $ly = 2.98$, 3.98, 4.30, and 4.96 $\pm$ 0.06 mm, respectively.

B. Parameter Sensitivity Coefficient

The analysis of sensitivity coefficients is a powerful tool for understanding the physical behavior of the problem.[19] The sensitivity coefficients show the variation of the transmittance or reflectance with respect to the absolute value of the parameters. Their comparison is not very easy when the parameters do not have the same units (which is often the case). Then for comparison, it is preferable to study the normalized dimensionless sensitivity coefficients, defined as: $X(i, j) = (\partial T_i / \partial p_j)(p_j / T_i)$, where T_i, $i = 1, 2$, represent hemispherical transmittance and hemispherical reflectance, respectively, and p_j, $j = 1, 11$, represent all of the parameters involved in the model δ, fs, b, b_{max}, and $\rho_{\lambda k}$, $k = 1, 7$.

Sensitivity coefficients for three specimen thickness ($ly = 2.98$, 3.98, and 4.96 mm) are studied (Figs. 2–5). Note that sensitivity coefficients of δ, fs, b, and b_{max} are nearly constant with the wavelength. These parameters are correlated. The sensitivity coefficient of δ is much larger than the others for the forward direction. On the contrary, for the forward direction, reflectivity sensitivity coefficients are nearly zero. They are large only for the backward direction and for the wavelength corresponding to the reflectivity identified (this explains the peak of the sensitivity coefficient). For the backward direction, they are the same for the three different thickness. For example, the sensitivity coefficient of $\rho_{\lambda 5}$ is shown in Fig. 4, the sensitivity coefficient of the other reflectivities $\rho_{\lambda i}$ are nearly the same but the peaks are shifted. For the backward direction, the sensitivity coefficients of b, b_{max}, and fs are nearly null for the three samples of different thicknesses (Fig. 5). Thus, the fs parameter and the reflectivities do not seem to be correlated.

The influence of the sample thickness on the sensitivity coefficient is studied. For the thinner sample (2.98 mm), the sensitivity coefficient of porosity is not negligible for the backward direction, contrary to the thicker sample (Fig. 5). Thus, an error in porosity can introduce an error in the identified reflectivities. Note that the sensitivity coefficients of the reflectivities are nearly the same for the

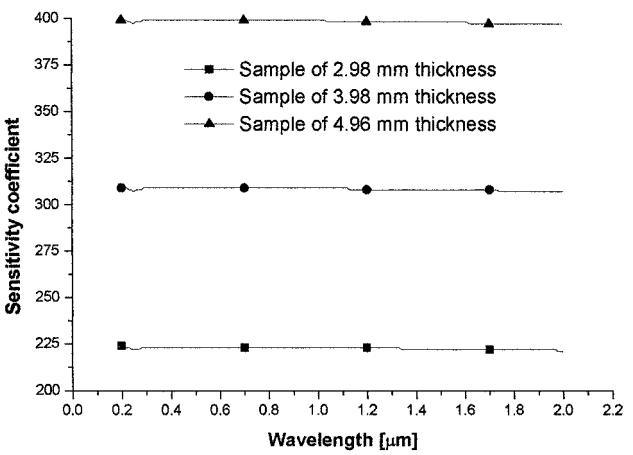

Fig. 2 Normalized sensitivity coefficient of porosity δ for forward direction (hemispherical transmittance).

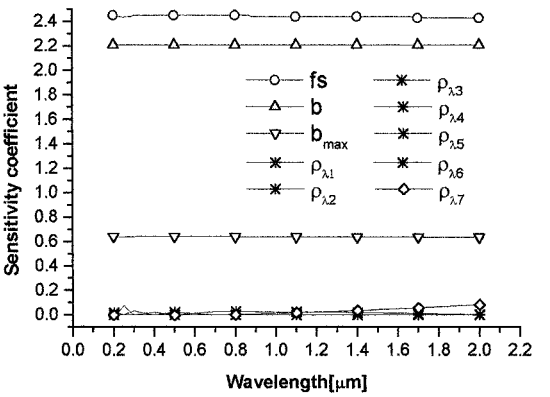

2.98-mm-thick sample

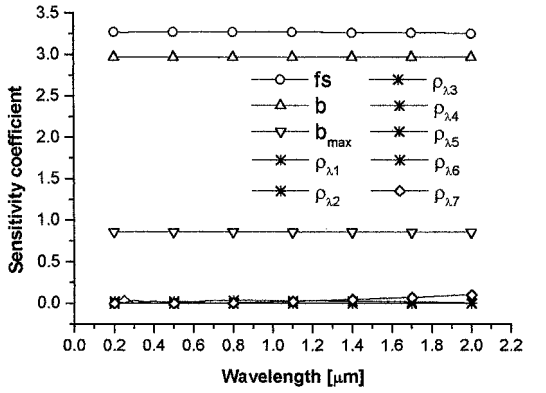

3.98-mm-thick sample

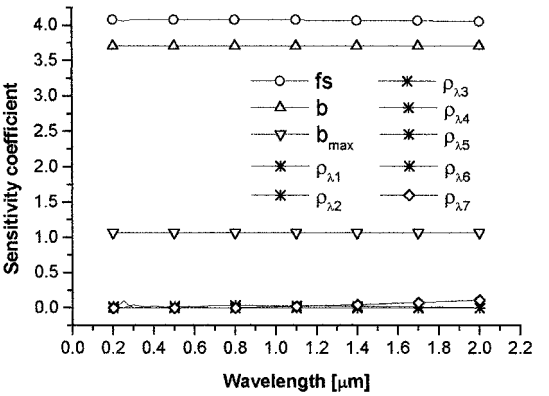

4.96-mm-thick sample

Fig. 3 Normalized sensitivity coefficient of parameters except δ for forward direction (hemispherical transmittance).

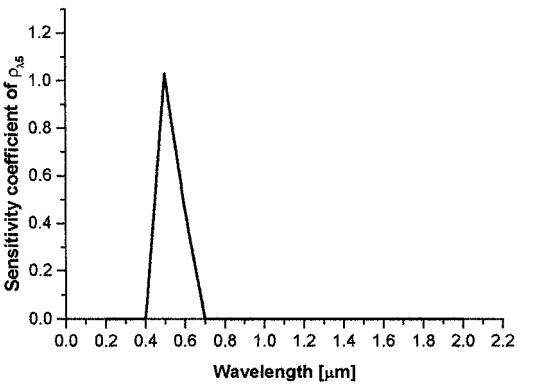

Fig. 4 Normalized sensitivity coefficient of reflectivities $\rho_{\lambda 5}$ for backward direction (hemispherical reflectance): samples 2.98, 3.98, and 4.96 mm thick.

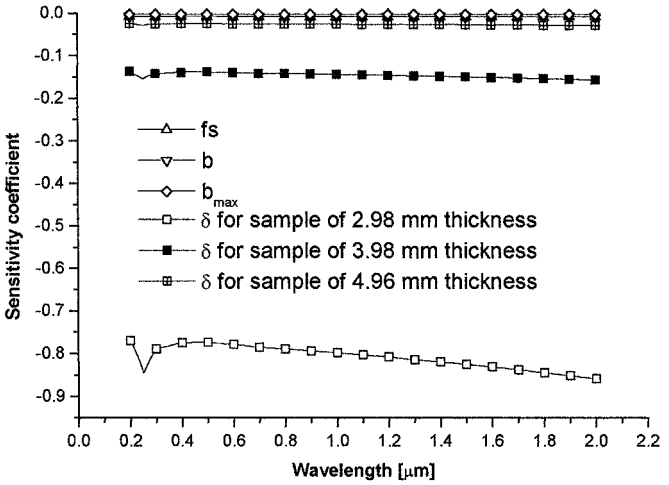

Fig. 5 Normalized sensitivity coefficient of parameters: porosity δ, fs, b, and b_{max} for backward direction (hemispherical reflectance) for samples of different thicknesses; sensitivity coefficient of fs, b, and b_{max} are nearly the same for the three thicknesses; they are nearly null.

three thicknesses. On the contrary, the sensitivity coefficients of δ, fs, and b seem to be larger for thicker thicknesses. As a result only the three thicker sample are used (3.98, 4.30, and 4.96 mm) to estimate the parameters.

C. Identification Results

For each specimen i, $i = 1, 3$, of different thickness ($ly = 3.98$, 4.30, and 4.96 mm, respectively) the fraction fs and the hemispherical reflectivity ρ_λ are identified from hemispherical transmittances and reflectances by using the parameter identification method described in Sec. III. Then these results, $(\rho_\lambda, fs)_i$, $i = 1, 3$, are used to calculate the average over the three specimens that gives the value of the hemispherical reflectivity ρ_λ and the fraction fs corresponding to the foam carbon studied. The mean square deviation of the identified values ρ_λ and fs are also calculated.

Results of fs value are given as follows. The fs identified from hemispherical measurements (0.2–2.1 μm) with 98.75% porosity is $fs = 0.337 \pm 0.014$. The value obtained is compared with the one obtained by Baillis et al.[3] for the same foam, from the directional–directional measurements for the wavelength region [2–15 μm]; the fs identified value is 0.335 ± 0.008. The two fs values are nearly the same. Therefore, the predictive model seems to be appropriate. To better validate the method, the value of fs has also been measured from microscopic analysis and is 0.60 ± 0.05. Note, however, that the value of fs obtained in this way is much larger than the values of fs identified. This can be explained from uncertainties on porosity. Indeed, an error on porosity introduces a large error on the identified fs value. For a porosity of $\delta - \Delta\delta = 97.97\%$, the identified fs value obtained from hemispherical measurements is $fs = 0.56 \pm 0.02$, and so this new value is closer to the one obtained from microscopic analysis. Moreover, the mean square deviation in porosity is obtained from six measurements, but the technique of measurement is the same. In reality the uncertainty in porosity is larger. On the other hand, it has been verified that a variation in the porosity induces neither a variation on the identified reflectivity nor a variation on the extinction coefficient β. Thus, radiative properties obtained from identified values are the same for porosity of 98.75% and 97.97%. These results can be explained from the sensitivity coefficients. Sensitivity of reflectivities is large only for the backward direction, and for this direction, sensitivity to the others parameters is very weak. Therefore, values of fs and porosity do not influence reflectivities identified. Moreover, fs and δ are correlated, and so a variation of porosity induces a variation of fs and leads to the same extinction coefficient β.

For three different types of carbon foam of different porosity ($\delta = 97.5$, 98.75, and 98.2) the fs value measured lies between 0.54 and 0.66. This confirms that fs value is around $\frac{2}{3}$.

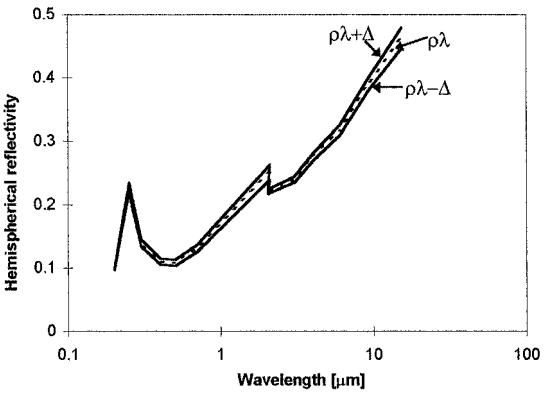

Fig. 6 Identified carbon hemispherical reflectivity plus or minus the standard deviation ($\rho_\lambda \pm \Delta$).

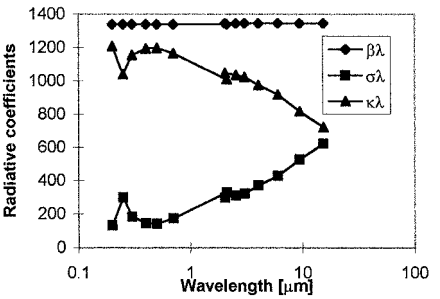

Fig. 7 Radiative coefficients of carbon foam.

The average values of the hemispherical reflectivity of carbon plus or minus mean square deviation are presented in Fig. 6. Values for the wavelength region 0.2–2.1 μm correspond to results obtained from hemispherical measurement of this work. Those for the region 2–15 μm correspond to values obtained by Baillis et al.[3] from directional–directional measurements. Notice that the measurements do not match exactly; directional–directional measurement leads to values just a little weaker than the hemispherical. This difference between the two approaches is probably due to the inaccuracy of the alignment of the goniometric device necessary for directional–directional measurements, the alignment of this device being particularly difficult.

The radiative properties of the foam are calculated from average values of fs and ρ_λ and from the prediction model neglecting diffraction [Eqs. (1) and (2)]; they are shown in Fig. 7. Notice that for the wavelength region 0.2–2.1 μm the scattering coefficient is much smaller than the absorption coefficient. In this region, such a medium is weakly scattering when diffraction is neglected. This is not the case for higher infrared wavelengths.

The theoretical value of transmittance and reflectance can be deduced from radiative properties calculated from average values of fs and ρ_λ. Experimental and theoretical results are in good agreement. Results for the 4.30-mm-thick sample are shown in Figs. 8 and 9. The abrupt change at the wavelength 0.8 μm in Fig. 8 is because light sources and detectors of the spectrometer Lambda 900 are different for the wavelength ranges 0.2–0.8 μm and 0.8–2.1 μm. Results are noisier in the wavelength region 0.8–2.1 μm.

D. Guarded Hot-Plate Results

This method consists of measuring the heat flux from a flat sample. The sample is heated by contact with a flat resistor of graphite 70 mm wide and 120 mm long. The temperature of the two faces (hot and cold) are measured by small diameter thermocouples. Experimental uncertainties in the guarded hot-plate device measurements are the following: 1) There are uncertainties about the temperatures of the hot and cold faces that are due to the inaccuracy of the location of thermocouples and to the thermal gradient between the center and the edges of faces. This error is estimated to be less than 8%. 2) There is uncertainty about the thermal flux; the inaccuracy is less than 5%.

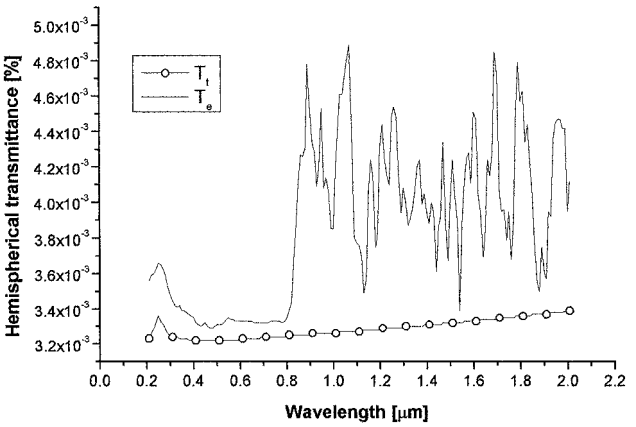

Fig. 8 Hemispherical transmittance for carbon foam sample 4.30 mm thick for normal incidence; experimental T_e and theoretical T_t results.

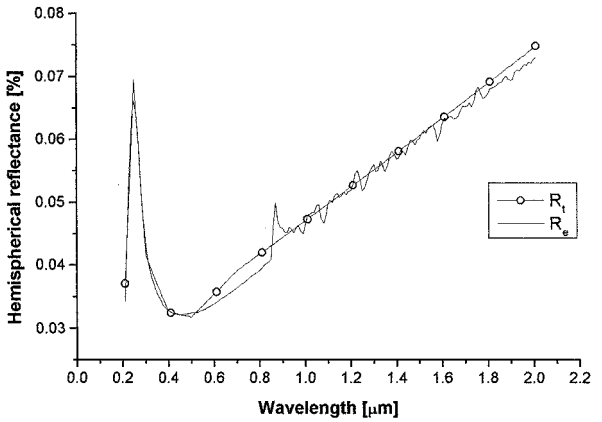

Fig. 9 Hemispherical reflectance for carbon foam sample 4.30 mm thick for normal incidence; experimental R_e and theoretical R_t results.

3) There is uncertainty about the thickness sample; the inaccuracy is less than 1%. 4) There is uncertainty due to the side thermal losses. Numerical simulations have proved that the inaccuracy is less than 1%.

Inasmuch as the temperatures are higher than 1000 K, the radiative transfer is much larger than the conduction heat transfer. Thus, the contact resistances between the plate and the foam are neglected. As a result the global error in the total conductivity measured is less than 15%.

Foam insulation is usually thick enough to be considered as optically thick. Thus, the radiative flux can be approximated by the Rosseland equation introducing a radiative conductivity[13–15]:

$$k_r = \frac{16n^2\bar{\sigma}T^3}{3\beta_R} \tag{4}$$

where $\bar{\sigma}$ is the Stefan–Boltzmann constant and n is the effective index of refraction, which can be taken $n = 1$ because the foam porosity is very high (98.75%).

Here, β_R is the Rosseland mean extinction coefficient defined by the following relation:

$$\frac{1}{\beta_R} = \int_0^\infty \frac{1}{\beta_\lambda^*}\frac{\partial e_{b\lambda}}{\partial e_b}\,\mathrm{d}\lambda \tag{5}$$

where e_b is the blackbody radiative emissive power. The Rosseland approximation is valid when the medium absorbs and scatters isotropically. To take into account the foam anisotropic scattering, a weighted spectral extinction coefficient β_λ^* is used[15]:

$$\beta_\lambda^* = \kappa_\lambda + \sigma_\lambda^*, \qquad \sigma_\lambda^* = \sigma_\lambda(1 - \langle\cos\theta\rangle_\lambda)$$

$$\langle\cos\theta\rangle_\lambda = 0.5\int_{-1}^{1} P_\lambda(\theta)\cos\theta\,\mathrm{d}(\cos\theta) \tag{6}$$

Table 1 Test 1, 15-mm-thick[a] sample

	Conductivity, $WK^{-1}\,m^{-1}$		
Total results	T_0 = 1038 T_1 = 356	T_0 = 1708 T_1 = 505	T_0 = 2227 T_1 = 764
Experimental	0.23	0.52	1.01
Theoretical	0.23	0.52	1.03

[a]Surface temperatures in degrees Kelvin.

Table 2 Test 2, 10-mm-thick[a] sample

	Conductivity, $WK^{-1}\,m^{-1}$		
Total results	T_0 = 1044 T_1 = 375	T_0 = 1726 T_1 = 585.5	T_0 = 2228 T_1 = 917
Experimental	0.24	0.59	1.17
Theoretical	0.23	0.56	1.12

[a]Surface temperatures in degrees Kelvin.

The total conductivity includes the three independent mechanisms: conduction through the gas, conduction through the solid material forming the cell, and thermal radiation[13–15]:

$$k_t = k_{\text{gas}} + k_{\text{solid}} + k_r \tag{7}$$

The gas is nitrogen. Its conductivity is defined by the following relation:

$$k_{\text{gas}} = k_0\left(1 + \frac{C}{273}\right)\frac{\sqrt{T/273}}{(1 + C/T)} \tag{8}$$

where $k_0 = 0.0242$ W/mK and $C = 161$ K. T is in degrees Kelvin.

Comparison Between Experimental and Theoretical Results

Experimental total conductivities are measured for two foam specimens 10 and 15 mm thick submitted to different surface temperatures (Tables 1 and 2). The Rosseland mean extinction coefficient and solid conductivity were determined from the guarded hot-plate measurements results. The solid phonic conductivity obtained is

$$k_{\text{solid}} = 93 \pm 8(10^{-3}\,\mathrm{Wm^{-1}K^{-1}}) \tag{9}$$

A Rosseland mean extinction coefficient can be calculated from the radiative properties of the predictive model and from Eq. (5) by using the average value of fs obtained from the two types of measurement, $fs = 0.336 \pm 0.011$, and the reflectivity obtained for the domain of wavelength of 0.2–15 μm. Recall (Sec. IV.C) that if a porosity of $\delta - \Delta\delta = 97.97\%$ and an identified values of fs equal to 0.56 are used, the radiative properties obtained are the same. For the same surface temperature as in the guarded hot-plate measurement, a Rosseland mean extinction is calculated and an average value with a mean square deviation is deduced. A good agreement is observed between the experimental and calculated Rosseland mean extinction coefficients, the relative difference being 2% (Table 3). Because the mean square deviation is weak, it can be verified that the Rosseland mean extinction coefficient is weakly dependent on temperatures.

Experimental results of total conductivity are compared with theoretical results obtained by using the experimental value of k_{solid} [Eq. (9)] and radiative properties obtained from the predictive model. Results of total conductivity for two tests are shown in Tables 1 and 2. For these two cases, experimental and theoretical total conductivity and conduction conductivity are shown as a function of the hot face temperature (Fig. 10). It can be verified that at high temperatures, radiative transfer is preponderant. Experimental and theoretical conductivities are in good agreement: Deviations are less than 6.5%; they are smaller than the experimental uncertainties given by the guarded heat plate device, which are 15%. Thus, these results confirm that the predictive model is appropriate to determine foam radiative properties.

Table 3 Value of β_R for the carbon foam sample

Results	$\beta_R \pm \Delta$, m^{-1}	$(\beta_R - \beta_{R\exp})/\beta_{R\exp}$, %
Guarded hot plate measurements	1453 ± 43	——
Radiative predictive model ρ_λ fs identified	1483 ± 19	2.1
Radiative predictive model $\rho_\lambda - \Delta$	1480 ± 17	1.8
Radiative predictive model $\rho_\lambda + \Delta$	1486 ± 19	2.3
Radiative predictive model $fs - \Delta$	1539 ± 20	5.9
Radiative predictive model $fs + \Delta$	1430 ± 18	1.6
Radiative predictive model $\sigma = 0$, $fs = \frac{2}{3}$	743	48.9
Radiative predictive model $\sigma = 0$, $fs = 0.6$	812	44.1
Radiative predictive model $\sigma = 0$, $fs = 0.336$ (identified)	1331	8.4

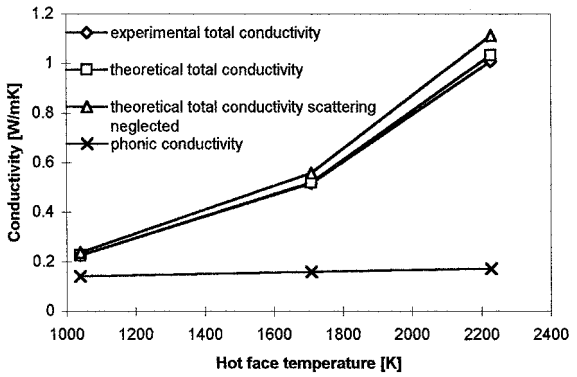

15-mm-thick sample

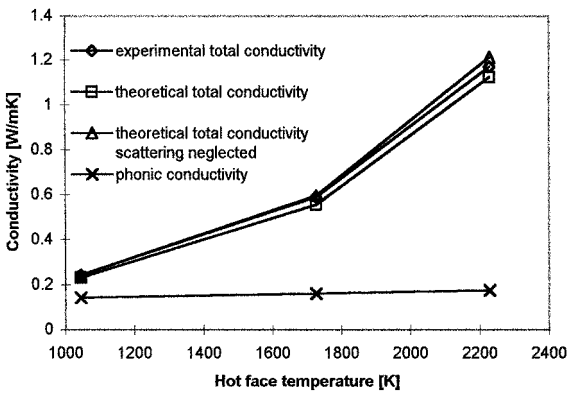

10-mm-thick sample

Fig. 10 Theoretical and experimental conductivity for two samples 15 and 10 mm thick.

Note that the conductivities obtained from the Rosseland approximation have been compared with those obtained from the discrete ordinates method[17]; the deviations were very weak, they are less than 2%. Therefore, because the optical thickness is larger than 10, the Rosseland approximation is valid.

Influence of the Uncertainties on the Carbon Hemispherical Reflectivity ρ_λ

Values of β_R obtained from the radiative predictive model with carbon hemispherical reflectivity plus and minus mean square deviation ($\rho_\lambda + \Delta$, $\rho_\lambda - \Delta$) are given on Table 3. The relative difference is around 2%.

Influence of the Uncertainties in the fs Values

Values of β_R obtained from the radiative predictive model with the fraction fs plus and minus mean square deviation ($fs + \Delta$, $fs - \Delta$ with $\Delta = 0.011$) are also shown on Table 3. The relative differences are less than 6%. It is shown that the influence of uncertainties of the carbon hemispherical reflectivity on β_R is weaker than the one of fs.

Comparison with Simpler Model

In previous work, Glicksman et al.[13] neglected the scattering by struts and considered that $fs = \frac{2}{3}$. Note the β_R can be calculated from this simpler model, but the relative difference in β_R is almost 50% (Table 3).

If scattering is neglected and the value of fs is measured from microscopic analysis ($fs = 0.6$), then the relative difference in β_R is 44% (Table 3).

If scattering is neglected and the fs value is identified ($fs = 0.336$) the relative difference in β_R decreases 8% (Table 3).

These results show that the use of a radiative model that does not take into account the scattering leads to relative difference in β_R of 8%. Probably a higher difference would be obtained for a higher reflectivity. The large relative difference in β_R obtained when fs is not identified but measured is probably due to the uncertainties in the porosity.

Theoretical results of total conductivity obtained by neglecting scattering are shown as a function of the hot face temperature in Fig. 10. Relative deviations with respect to experimental values are less than 8%.

V. Conclusion

An approach to determine radiative properties of open cell foam is described. The predictive model of Doermann and Sacadura[15] is used, but diffraction phenomena are neglected. Radiative properties are determined as a function of b, $b_{\max}$, δ, fs, and ρ_λ. Parameters b, $b_{\max}$, and δ are obtained from microscopic analysis. Parameters fs and ρ_λ are determined from an identification method by using hemispherical transmittance and reflectance measurements in the wavelength region 0.2–2.1 μm.

This approach is completed and compared with that of Baillis et al.[3] using directional–directional transmittance and reflectance measurements in the wavelength range 2–15 μm for carbon foam samples of 98.75% porosity.

1) The same value of fs is obtained from the two approaches. This is consistent; indeed, fs is a parameter independent of the wavelength. This shows the good behavior of the model and confirms that diffraction phenomena can be neglected.

2) The experimental results of transmittance and reflectance and the theoretical results deduced from radiative properties are globally in good agreement.

3) The two approaches give nearly the same results, but hemispherical measurements are easier to implement, and, as a result, they are more appropriate.

4) Radiative properties of carbon foam of 98.75% porosity have been determined in a wavelength region from visible to infrared.

Radiative conductivities have been calculated from these radiative properties. Experiments on a guarded hot-plate-type device permitted the comparison of the experimental and theoretical conductivities. The good agreement observed confirms that the proposed model is appropriate to predict the radiation heat transfer in such material. As shown by the sensitivity coefficient analysis this model requires very accurate knowledge of the porosity; consequently, because it is difficult to measure directly the porosity with precision, it is recommended to identify its value.

Acknowledgments

The authors acknowledge Aerospatiale–Etablissement d'Aquitaine for support of this project. They also wish to thank ONERA for the guarded hot-plate measurements.

References

[1] Viskanta, R., and Mengüç, M. P., "Radiative Transfer in Dispersed Media," *Applied Mechanics Review*, Vol. 42, No. 9, 1989, pp. 241–259.

[2]Baillis-Doermann, D., and Sacadura, J. F., "Thermal Radiation Properties of Dispersed Media: Theoretical Prediction and Experimental Characterization," *Radiative Transfer II*, edited by P. Mengüç, Begell House, New York, 1998, pp. 1–38.

[3]Baillis, D., Raynaud, M., and Sacadura, J. F., "Spectral Radiative Properties of Open Cell Foam Insulation," *Journal of Thermophysics and Heat Transfer*, Vol. 13, No. 3, 1999, pp. 292–298.

[4]Fu, X., Viskanta, R., and Gore, J. P., "A Model for the Volumetric Radiation Characteristics of Cellular Ceramics," *International Communications in Heat and Mass Transfer*, Vol. 24, No. 8, 1997, pp. 1069–1082.

[5]Hale, M. J., and Bohn, M. S., "Measurements of the Radiative Transport Properties of Reticulated Alumina Foams," *Proceedings of the ASME/ASES Joint Solar Energy Conference*, edited by A. Kirkpatrick and W. Worek, American Society of Mechanical Engineers, New York, 1993, pp. 507–515.

[6]Hendricks, T. J., and Howell, J. R., "Absorption/Scattering Coefficients and Scattering Phase Functions in Reticulated Porous Ceramics," *Journal of Heat Transfer*, Vol. 118, Feb. 1996, pp. 79–87.

[7]Hendricks, T. J., and Howell, J. R., "New Radiative Analysis Approach for Reticulated Porous Ceramics Using Discrete Ordinates," *Journal of Heat Transfer*, Vol. 118, Nov. 1996, pp. 911–917.

[8]Hsu, P. F., and Howell, J. R., "Measurements of Thermal Conductivity and Optical Properties of Porous Partially Stabilized Zirconia," *Experimental Heat Transfer*, Vol. 5, 1992, pp. 293–313.

[9]Kamiuto, K., "Study of Dul'nev's Model for the Thermal and Radiative Properties of Open-Cellular Porous Materials," *Japan Society of Mechanical Engineers International Journal, Series B*, 1997, pp. 577–582.

[10]Kamiuto, K., and Matsushita, T., "High-Temperature Radiative Properities of Open-Cellular Porous Materials," *Heat Transfer 1998: Proceedings of the 11th International Heat Transfer Conference*, edited by J. S. Lee, Taylor and Francis, Vol. 7, 1998, pp. 385–390.

[11]Mital, R., Gore, J. P., and Viskanta, R., "Measurements of Radiative Properties of Cellular Ceramics at High Temperatures," *Journal of Thermophysics and Heat Transfer*, Vol. 10, No. 1, 1996, pp. 33–38.

[12]Skocypec, R. D., Hogan, R. E., Jr., and Muir, J. F., "Solar Reforming of Methane in a Direct Absorption Catalytic Reactor on a Parabolic Dish: II—Modeling and Analysis," *Proceedings of the ASME–ISME 2nd International Solar Energy Conference*, edited by T. R. Mancini et al., Solar Energy Div., American Society of Mechanical Engineers, New York, 1991, pp. 303–310.

[13]Glicksman, L. R., Marge, A. L., and Moreno, J. D., "Radiation Heat Transfer in Cellular Foam Insulation," *HTD, Developments in Radiative Heat Transfer ASME*, Vol. 203, 1992, pp. 45–54.

[14]Kuhn, J., Ebert, H. P., Arduini-Chuster, M. C., Büttner, D., and Fricke, J., "Thermal Transport in Polystyrene and Polyurethane Foam Insulations," *International Journal of Heat and Mass Transfer*, Vol. 35, No. 7, 1992, pp. 1795–1801.

[15]Doermann, D., and Sacadura, J. F., "Heat Transfer in Open Cell Foam Insulation," *Journal of Heat Transfer*, Vol. 118, Feb. 1996, pp. 88–93.

[16]Van De Hulst, H. C., *Light Scattering by Small Particles*, Wiley, New York, 1957, pp. 103–113.

[17]Doermann, D., "Modélisation des transferts thermiques dans des matériaux semi-transparents de type mousse à pores ouverts et prédiction des propriétés radiatives," Doctoral Thesis, No. Order 95ISAL0010, Institut National des Sciences Appliquées, Lyon, France, Jan. 1995.

[18]Beck, J. V., and Arnold, K. J., *Parameter Estimation in Engineering and Science*, Wiley, New York, 1977, Chap. 7.

[19]Raynaud, M., "Strategy for Experimental Design and the Estimation of Parameters," *High Temperatures–High Pressures*, No. 31, 1999, pp. 1–15.